International Journal of Hybrid Information Technology
Vol.8, No.3 (2015), pp.273-286
http://dx.doi.org/10.14257/ijhit.2015.8.3.24

Study on Matrix Converter Based on Input Damping Filter

Hanying Gao, Wei Yang, Duanzeng Liu and Weili Li

School of Electrical and Electronic Engineering,
Harbin University of Science and Technology, Harbin, China
E-mail: ghyljt@sina.com

Abstract

Compared with traditional PWM converters, the matrix converter with high development potential has many advantages, such as simpler structure, better controllable performance, higher power factor, less harmonic pollution to the grid and no large-capacity DC capacitor. Currently, among a variety of modulation algorithms for the matrix converter, the double SVPWM control algorithm is the most mature. This paper analyzes the double SVPWM control strategy and the realization of the variable frequency and variable voltage. Aiming at the pollution problem from the input side current harmonics to grid, a damping LC filter is designed in the input side. However, the input filter will cause reactive power increase and result in power factor decrease of the grid side. To ensure the unit power factor of the grid side, this paper deduces the relationship between the actual power factor angle of the grid side and damping filter. By adjusting the setting value of the input side power factor, the unit power factor of the grid side can be obtained. Simulation results verify the validity of the theoretical analysis.

Keywords: *double SVPWM control algorithm, variable frequency and variable voltage, LC damping filter, grid side unit power factor, matrix converter*

1. Introduction

Matrix converter (MC) is a novel AC-AC power conversion device with characteristics of simple topology, controllable grid power factor, two-way energy flow, sinusoidal input current, sinusoidal output voltage and without intermediate DC energy storage device, *etc*., [1, 2], it has drawn people's great attention. For the characteristics of small current harmonic and reactive power compensation to grid, the MC shows a broad application prospect in many fields, such as motor driving and wind power generation, etc.

In order to obtain the sine wave input and less the input harmonic current to the grid, the MC must employ the input filter, which was commonly a LC topology. Paper [3], proposed input LC filter, the LC circuit was a second-order non-damping system, which will cause the instability of filter system under the continuous interference from the output side harmonic current. Paper [4], proposed two-stage input LC filter circuit, but the two-stage LC filter increased the complexity and cost of the input filter. Paper [5], proposed the integrated filter on the input and output side, by coupling the input and output filter, the common-mode voltage generated from motor drive can be reduced to zero, but this method added the output filter, increased the power consumption and volume of the converter, the designing of the device was more complex. Paper [6], proposed the genetic algorithm to obtain the filter parameters through optimizing multiple objectives optimization function, which achieved a good simulation results, but the computation method was quite complex and hard to realize.

ISSN: 1738-9968 IJHIT

In view of the above situation, this paper gives a damping LC filter on the input side. With the increase of damping coefficient, the input phase-current oscillations will be inhibited easily. Aiming at the problem that filter will lead to a decrease of grid side power factor, a method adjusting set value of gird side power factor is proposed in this paper. In the meantime, the simulation system with double space vector modulation, damping LC filter and the grid side power factor adjustment are established, and simulation results verify the validity of the theoretical analysis.

2. The Basic Principle of Matrix Converter

The MC with three-phase to three-phase consists of nine power devices with two-way blocking and self turn-off ability, which formed 3*3 switches array. Each output phase connects a three-phase input terminal by a two-way switch respectively. Through a certain modulation strategies to control on-off of the power devices, the MC can realize the simultaneous modulation of output voltage and input current, and at the same time realize variable frequency, variable voltage and high power factor operation. The MC topology structure is shown in Figure 1.

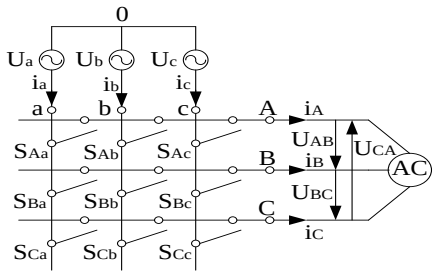

Figure 1. MC Topology with Three-phase to Three-phase

Currently, among a variety of modulation algorithms of matrix converter, double SVPWM control algorithm is the most mature, which makes the MC topology equivalent to AC-DC-AC structure (as shown in Figure 2). With the advanced high-frequency rectifier and inverter technology, we can realize the overall control of the MC.

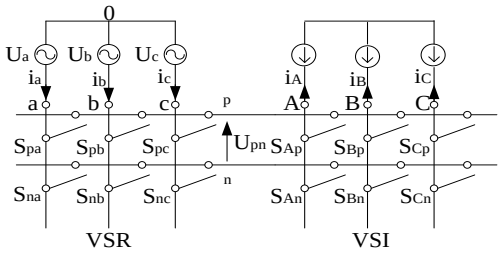

Figure 2. Topology with the MC Equivalent to AC-DC-AC Topology

3. Double SVPWM Control

The MC SVPWM with three-phase to-three phase is an indirect transformation method [7]. By the double PWM modulation technology, the MC can be equivalent to a virtual AC-DC-AC topology structure (as shown in Figure 2), the virtual rectifier side and the virtual inverter side adopt space vector modulation algorithm respectively. On the input side, the current shares the same (or adjustable) phase with grid voltage, that's to say, we can achieve

adjustable input power factor. In the algorithm, the DC segment can be eliminated through an equivalent principle of intermediate DC voltage and current, finally, two virtual sides will be combined to achieve the overall control, also known as the double space voltage vector method.

The SVM modulation of output line voltage of the virtual inverter is shown in Figure 3. Assumes that the DC voltage supply of VSI U_{PN} equals to U_{dc}, and only six combinations generate the non-zero voltage vectors, two combinations generate the zero vectors, the output line-voltage U_O can be defined as:

$$U_o = \frac{2}{3}(U_{AB} + U_{BC}e^{+j120^\circ} + U_{CA}e^{-j120^\circ}) \tag{1}$$

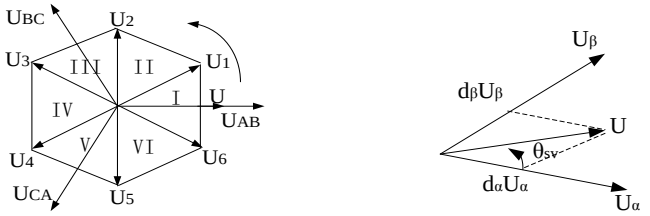

(a) Output line-voltage SVPWM (b) output voltage vector composite

Figure 3. SVPWM Diagram with VSI Inverter

At a certain moment, the output line-voltage space vector is composted by two adjacent non-zero vector U_α, U_β and a zero vector U_0, the functional time of every vector by the sine theorem can be deduced as:

$$\begin{cases} d_\alpha = T_\alpha / T_s = m_v \sin(60^\circ - \theta_{sv}) \\ d_\beta = T_\beta / T_s = m_v \sin(\theta_{sv}) \\ d_{0v} = T_{0v} / T_s = 1 - d_\alpha - d_\beta \end{cases} \tag{2}$$

where d_α, d_β, d_{0v} are duty ratios of voltage vector U_α, U_β, U_0 respectively, the m_v is the voltage modulation coefficient, and $0 \le m_v = \sqrt{3}\, U_{om}/U_{dc} \le 1$, T_α, T_β, T_{0v} are conducting time of switches, θ_{sv} is an angle between the output voltage vector and the sector initial position.

As shown in Figure 4, space voltage vector modulation of the input current for the virtual rectifier side is similar to that of VSI. Assume that the direct current i_P generated by VSR equals to I_{dc}, and only six combinations generate non-zero input current vectors, three combinations generate the zero vectors, U_{iPh} can be defined as:

$$U_{iPh} = \frac{2}{3}(U_{a0} + U_{b0}e^{+j120^\circ} + U_{c0}e^{-j120^\circ}) \tag{3}$$

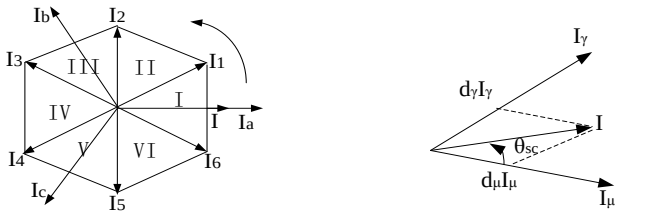

(a) Input phase-current SVPWM (b) input phase-current vector composition

Figure 4. SVPWM Diagram with VSR Rectifier

At a certain moment, the input phase-current space vector is composted by two adjacent non-zero vector I_μ, I_γ and a zero vector I_0, the functional time of every vector by the sine theorem can be deduced as:

$$\begin{cases} d_\mu = T_\mu / T_s = m_c \sin(60^\circ - \theta_{sc}) \\ d_\gamma = T_\gamma / T_s = m_c \sin(\theta_{sc}) \\ d_{0c} = T_{0c} / T_s = 1 - d_\mu - d_\gamma \end{cases} \tag{4}$$

Where d_μ, d_γ, d_{0c} are duty ratios of current vector I_μ, I_γ, I_0 respectively, the m_c is the current modulation coefficient, and $0 \le m_c = \sqrt{3}\, I_{im}/I_{dc} \le 1$, T_μ, T_γ, T_{0c} are conducting time of switches, θ_{sc} is an angle between the input current vector and the sector initial position.

VSR and VSI space vector modulation of the MC are independent of each other in the AC-DC-AC structure, so the integration is needed, namely calculate the five integrated duty ratios of the corresponding voltage and current within a PWM cycle. The integrated duty ratios corresponding to a combination of switches are respectively:

$$\begin{cases} T_1 = T_{\alpha\mu} = d_\alpha d_\mu T_s = d_{\alpha\mu} T_s = T_s m \sin(60^\circ - \theta_{sv}) \sin(60^\circ - \theta_{sc}) \\ T_2 = T_{\beta\mu} = d_\beta d_\mu T_s = d_{\beta\mu} T_s = T_s m \sin(\theta_{sv}) \sin(60^\circ - \theta_{sc}) \\ T_3 = T_{\alpha\gamma} = d_\alpha d_\gamma T_s = d_{\alpha\gamma} T_s = T_s m \sin(60^\circ - \theta_{sv}) \sin(\theta_{sc}) \\ T_4 = T_{\beta\lambda} = d_\beta d_\gamma T_s = d_{\beta\gamma} T_s = T_s m \sin(\theta_{sv}) \sin(\theta_{sc}) \\ T_0 = T_s - T_1 - T_2 - T_3 - T_4 \end{cases} \tag{5}$$

Where m is modulation coefficient of the MC, $m = m_v m_c$, often assumes the $m_c = 1$, $m = m_v$.

Double SVPWM control adopts the nine sections pulse width modulation. VSI and VSR integration will generate 36 kinds of switch states. To minimize the switching frequency and reduce the switching loss, optimal switching modulation sequence were given as follows [8]:

(1) When the sum of input current and output voltage space vector modulation sectors is an even number, the modulation sequence is:

$$d_{\beta\mu} \to d_{\alpha\mu} \to d_{\alpha\gamma} \to d_{\beta\gamma} \to d_0$$

(2) When the sum of input current and output voltage space vector modulation sectors is an odd number, the modulation sequence is:

$$d_{\alpha\mu} \to d_{\beta\mu} \to d_{\beta\gamma} \to d_{\alpha\gamma} \to d_0$$

(3) The strategy to choose a zero vector is to minimize the switch number as a benchmark.

4. Design of Input Filter

MC must utilize input filter to eliminate the input current harmonic, which avoid harmonic current pollute the grid. Because the MC is a BUCK topology, its outstanding advantage is the only need of a small input filter, while the input filter can avoid high-frequency harmonic effect from the grid to the MC.

The MC input filter is usually a LC circuit, as shown in Figure 5, L and C are respectively a inductance and capacitance of the input filter without damping resistance R. The input side current Ii of the converter is the PWM wave.

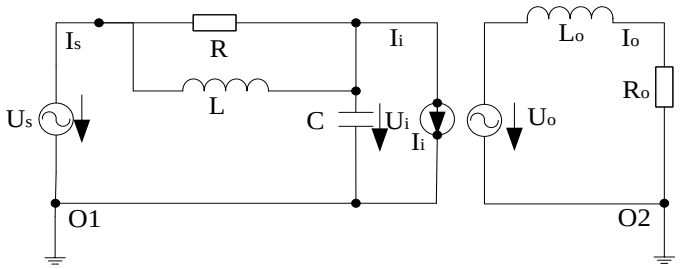

Figure 5. Single-phase Equivalent Circuit of MC

The relationship between voltage and current are obtained by Laplace transformation:

$$\begin{cases} U_s(s) - U_i(s) = sLI_s(s) \\ I_s(s) - I_i(s) = sCU_i(s) \end{cases} \tag{6}$$

Eliminating $U_i(s)$, transfer functions of input current, input voltage and output current are:

$$\begin{aligned} I_s(s) &= H_U(s)U_s(s) + H_I(s)I_i(s) \\ H_U(s) &= \frac{sC}{s^2LC+1} \\ H_I(s) &= \frac{1}{s^2LC+1} \end{aligned} \tag{7}$$

Apparently, from the above transfer functions, I_s has nothing to do with the output load characteristic and the power levels of the MC. $H_I(s)$ is the transfer function in correlation with the converter input side current I_i, which is mainly affected by the input current characteristics of the MC. We can find that the denominators of second-order transfer function between $H_U(s)$ and $H_I(s)$ are the same, their characteristic frequency ω_n are:

$$\omega_n = \frac{1}{\sqrt{LC}} \tag{8}$$

where resonant frequency, $f_r=\omega_n/2\pi$.

Since the resistance value of the filter inductance is small and can be ignored, the damping coefficient of LC filter is zero. Because input current of the MC is a sine PWM wave, there is a high harmonic content near the switching frequency. This PWM wave will contribute strong disturbance to the second-order LC circuit, which make the LC circuit to generate oscillation near the resonant frequency, cause a large amount of the current harmonics, affect stability and input-output performance of the MC. Set the parameters as follows: the filter inductance L=2.5mH, filter capacitance C=10uF, the output frequency 30Hz, the switching frequency 10kHz, resonance frequency 1006Hz, the simulation results are shown in Figure 6. Phase current of the grid side is with large harmonic and poor smoothness, and a large number of harmonics near resonance frequency can be seen from the spectrum diagram, which makes a large harmonic distortion and affects both the grid and converter.

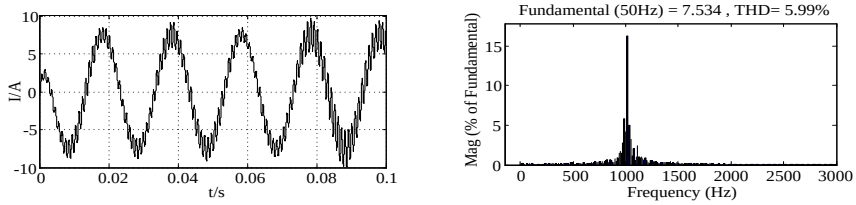

(a) input phase-current waveform (b) FFT analysis of input phase current

Figure 6. Input phase-current Analysis under the Non-damping Condition

The above introduction of the LC filter is a second-order non-damping system. Due to the continuous interference of the output side harmonic current will lead to instability of the filter system, while the increasing of damping coefficient can suppress the input phase-current oscillation. A damping input filter analysis method was stated as follows. Under the condition of the three-phase power balancing supply and three-phase balancing load, the MC with three phase to three phase can be equivalent to three single-phase power conversion device combination [9], as shown in Figure 5.

From the perspective of the input side, the power unit of the MC can be seen as a current source, from the perspective of the output side, the power unit of the MC can be seen as a voltage source. Relationships between voltage and current are obtained by Laplace transformation:

$$\begin{cases} U_s(s) - U_i(s) = \dfrac{sLR}{R+sL} I_s(s) \\ I_s(s) - I_i(s) = sCU_i(s) \end{cases} \tag{9}$$

Eliminating $U_i(s)$, the transfer function of input current and input voltage and output current are:

$$\begin{aligned} I_s(s) &= H_{Ud}(s)U_s(s) + H_{Id}(s)I_i(s) \\ H_{Ud}(s) &= \frac{s^2LC + sCR}{s^2RLC + sL + R} \\ H_{Id}(s) &= \frac{R + sL}{s^2RLC + sL + R} \end{aligned} \tag{10}$$

From the above equations, the second-order transfer functions of the denominator are the same, which the characteristic frequency ω_n and the damping coefficient ζ are:

$$\omega_n = \sqrt{\frac{1}{LC}} \ , \ \zeta = \frac{1}{2R}\sqrt{\frac{L}{C}} \tag{11}$$

With setting the damping resistance R=100Ω, holding other parameters constant and calculating the damping coefficient ζ=0.08, the simulation results are shown in Figure 7. Under the condition of increasing damping coefficient of the LC filter, the grid side phase-current harmonic is significantly reduced, with a better polished waveform compared to the input phase-current waveform of non-damping condition in Figure 6, what's more, a significantly lower harmonic distortion rate and a less harmonic contents near the resonant frequency can be seen from the spectrum diagram which indicates a lower oscillations of damping LC filter near the resonance frequency.

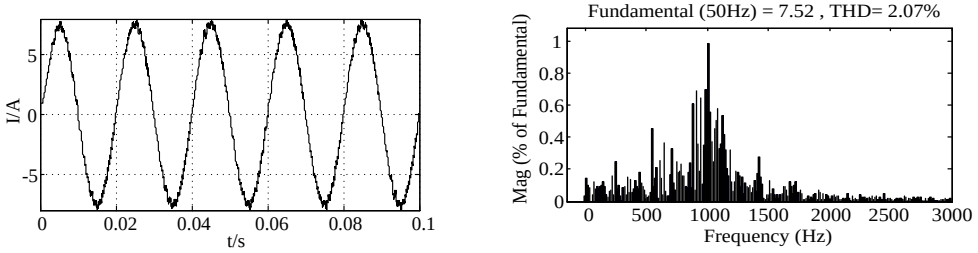

(a) Input phase-current waveform (b) FFT analysis of input phase-current

Figure 7. Input Phase-current Analysis on Increasing the Damping Coefficient

5. Realization of Variable Frequency and Variable Voltage

To maintain the motor flux Φ_m as a constant, the MC can control the ratio of output frequency and voltage. When adjusting the output voltage frequency f_0 from the rated 50Hz downwards, the output voltage amplitude must be reduced at the same time, which makes f_0/U_0=const. During the process of the output voltage, the voltage amplitude is controlled by modulation ratio m. During the simulation process, the change of the output voltage amplitude is desired with the change of output voltage frequency f_0, that is, we can choose the modulation ratio $m=f_0/50$ under the rated frequency. When adjusting the speed beyond the rated frequency, with the output frequency increasing, output voltage can't exceed the rated voltage, which should maintain the rated voltage at most. During the simulation process, the modulation ratio is setting to m=1.

Simulink/Lookup table module was adopted to control the modulation ratio with the change of the output frequency. Due to the relationship between the output phase voltage amplitude and the input phase voltage amplitude, we can know that the maximum voltage utilization rate can be up to 0.866.

$$U_{om} = \frac{\sqrt{3}}{2} m U_{im} \cos\varphi_i \tag{12}$$

The output line voltage amplitude is $U_o = \sqrt{3}\, U_{om}$, then

$$U_o = \frac{3}{2} m U_{im} \cos\varphi_i \tag{13}$$

As shown in Figure 8, the simulation results show that the change of the output frequency cause the change of the output line-voltage amplitude and modulation ratio.

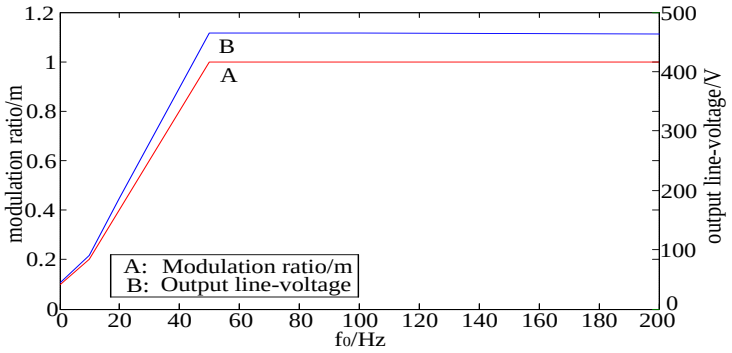

Figure 8. Relationships among Output Frequency, M and Output Line Voltage

6. Grid Side Power Factor Adjustment Method

In order to reduce the current harmonic contents into the grid side, usually introducing an input filter at the front-end of the converter, while the filter will affect the grid side power factor. In order to guarantee the grid side unit power factor, the power factor set value on the input side of the converter should be adjusted to offset the power factor angle deviation [10].

The damping LC filter structure of the input side is shown in Figure 9, among them U_s, I_s are the input voltage and current of the grid side, U_{in}, I_{in} are the voltage and current of the input side of the converter.

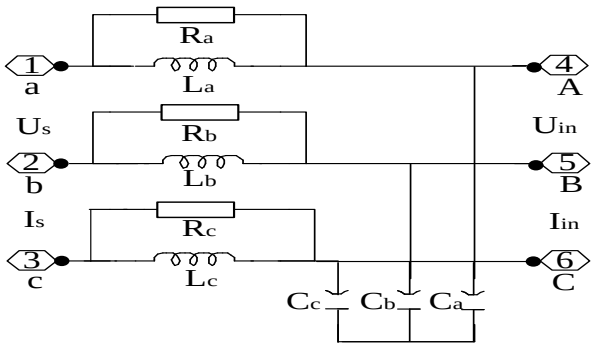

Figure 9. Input Side LC Filter

Considering U_{in} is possibly being affected by the switch process, set U_s as a reference value. Assuming $R_a=R_b=R_c=R$, $L_a=L_b=L_c=L$, $C_a=C_b=C_c=C$, $U_s=U_m\angle\alpha$, $I_{in}=I_m\angle(\alpha-\varphi)$, $I_s=I_x\angle\beta$. Through the analysis of the circuit, the following formulae can be obtained:

$$\begin{cases} U_s - U_{in} = \dfrac{j\omega_i LR}{j\omega_i L + R} I_s \\ U_{in} = \dfrac{1}{j\omega_i C}\left(I_s - I_{in}\right) \end{cases} \tag{14}$$

Eliminating U_{in}, substituting the specific expressions of each vector, and properly simplifying, we get

$$(j\omega_i CR - \omega_i^2 LC)U_m\angle\alpha + (j\omega_i L + R)I_m\angle(\alpha-\varphi) = (j\omega_i L + R - \omega_i^2 LCR)I_x\angle\beta \tag{15}$$

By the composition of the real and imaginary parts of each vector of the above formula (As shown in Figure 10), the simplification can be expressed as: A + B = C. Description: as shown in Figure 10(a), vector A is composed by vector A1 and A2, vector B is composed by vector B1 and B2, vector C is composed by vector C1 and C2. As shown in Figure 10(b), vector C is composed by vector A and B. Among them:

$$A1 = \omega_i^2 LCU_m\angle(\alpha+180^\circ), A2 = j\omega_i CRU_m\angle\alpha$$
$$B1 = RI_m\angle(\alpha-\varphi), B2 = j\omega_i LI_m\angle(\alpha-\varphi)$$
$$C1 = (R-\omega_i^2 LCR)I_x\angle\beta, C2 = j\omega_i LI_x\angle\beta$$

According to the above formulas, θ_1, θ_2, θ_3 of composition diagram of vector A, B and C can be obtained:

$$\theta_1 = \arctan\frac{\omega_i L}{R}, \theta_2 = \arctan\frac{\omega_i L}{R}, \theta_3 = \arctan\frac{\omega_i L}{R(1-\omega_i^2 LC)}$$

Substituting the parameters, which can obtain $\theta_1=\theta_2\approx\theta_3\approx 0^\circ$, for the convenience of calculation, the A, B and C are equivalent as follows:

$$A = \sqrt{(\omega_i CR)^2 + (\omega_i^2 LC)^2}U_m\angle(\alpha+90^\circ)$$
$$B = \sqrt{(\omega_i L)^2 + R^2}I_m\angle(\alpha-\varphi)$$
$$C = \sqrt{(\omega_i L)^2 + (R-\omega_i^2 LCR)^2}I_x\angle\beta$$

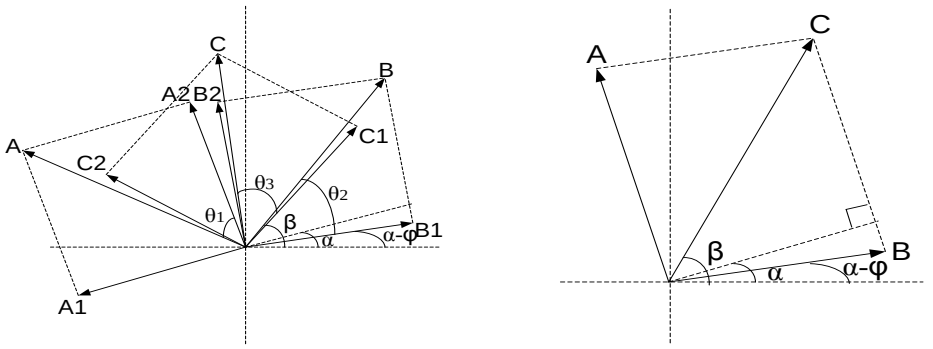

(a) Composition diagram of vector A, B and C (b) composition diagram of vector C

Figure 10. Vector Composition Diagram of Eq. (15)

According to the vector composition diagram, input power factor angle of the grid side is derived as follows:

$$\varphi' = \alpha - \beta = -\arctan\frac{A - B\sin\varphi}{B\cos\varphi} = -\arctan\frac{\sqrt{(\omega_i CR)^2 + (\omega_i^2 LC)^2}U_m - \sqrt{(\omega_i L)^2 + R^2}I_m \sin\varphi}{\sqrt{(\omega_i L)^2 + R^2}I_m \cos\varphi} \quad (16)$$

From the above equation, the actual grid side power factor angle φ' is related to the filter capacitance C, inductance L, resistance R, the grid side voltage amplitude U_m and current amplitude I_m, the input voltage angular frequency ω_i and the setting value of the input power factor angle φ.

Because the voltage amplitude of the grid side and angular frequency of the input voltage are fixed, while the change of the input filter will largely influence the power factor and current harmonic, and the input filter will generally take an appropriate value, which can be regarded as fixed. While the current amplitude of the grid side is affected by the output current of the converter, and the output current is affected by the output voltage, and the output voltage is affected by the output frequency, so the current amplitude of the grid side is affected by the output frequency, which is a not fixed value, therefore, the only method that can change the actual power factor angle of the grid side is by adjusting the setting value of the input power factor angle.

In order to guarantee the grid side as unit power factor, that input power factor angle of the grid side can be derived from the above equation ($\varphi'=\alpha-\beta$) which equals to 0, substitute the parameters, then obtain the given power factor angle of the theoretical adjustment of the input side of the converter. As Table 1 shows, when the given power factor of the input side of the converter is 1, the simulation output power factor of the grid side is generally equal to the given power factor of the theoretical adjustment of the input side of the converter. The tiny error is caused by the deviation of calculation.

Table 1. Comparison Results of Theoretical and Simulation Results

f_0/Hz	5	10	15	20	30	40	50	100	200
A	0.48	0.685	0.9	0.966	0.994	0.998	1	0.997	0.97
B	0.482	0.68	0.9	0.965	0.992	0.997	1	0.996	0.97

A: When the given power factor of the input side of the converter is 1, the simulation output power factor of the grid side before adjustment.

B: The given power factor of the theoretical calculation of the input side of the converter after adjustment.

7. System Simulation and the Result Analysis

Based on the above analysis, the established system simulation model of the MC by Matlab/Simulink is shown in Figure 11. The power supply adopts the balancing three-phase power supply (380V/50Hz), the switch matrix adopts the common collector two-way switch, the three-phase resistance and inductance load (L=18mH, R=10Ω) adopts the star connection, the control part adopts S-function (Uout_alpha_ beta, SVPWM, pulse_ out) to build simulation models.

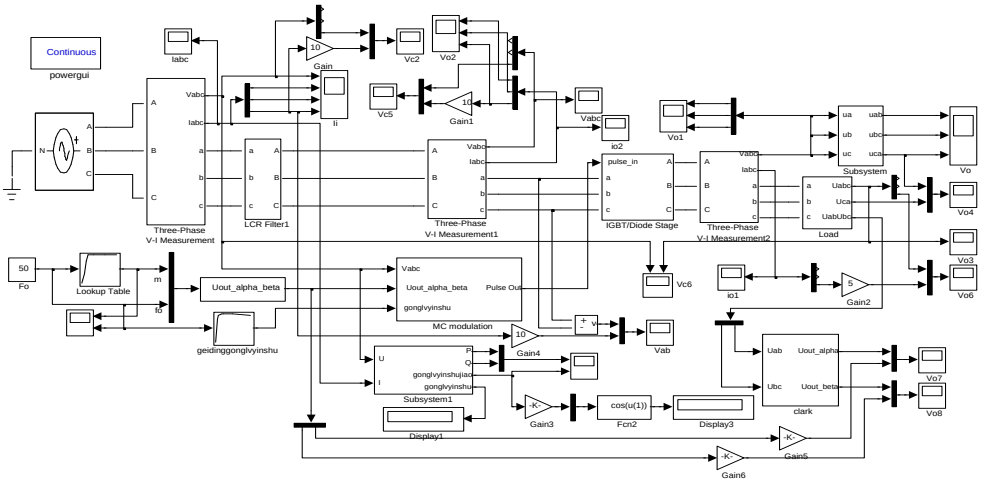

Figure 11. Simulation Model of MC System

S-function mainly completes the sector judgment, the duty ratio calculation, the calculation of 36 kinds of effective switch combination, the nine sections pulse width modulation and the lookup of the effective switch combination, *etc*., which is shown in Figure 12.

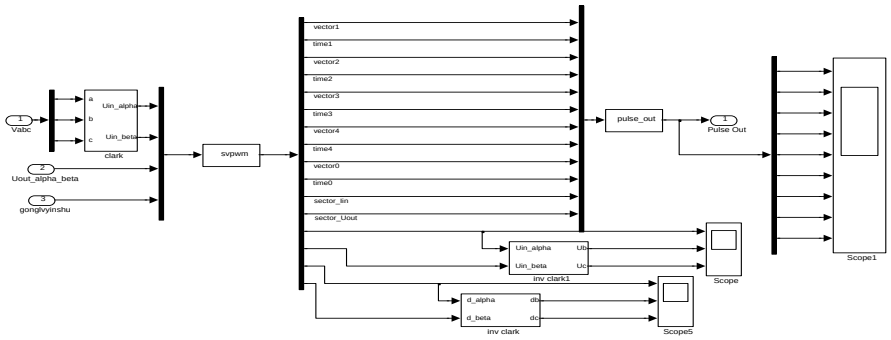

Figure 12. Simulation Diagram of MC control Section

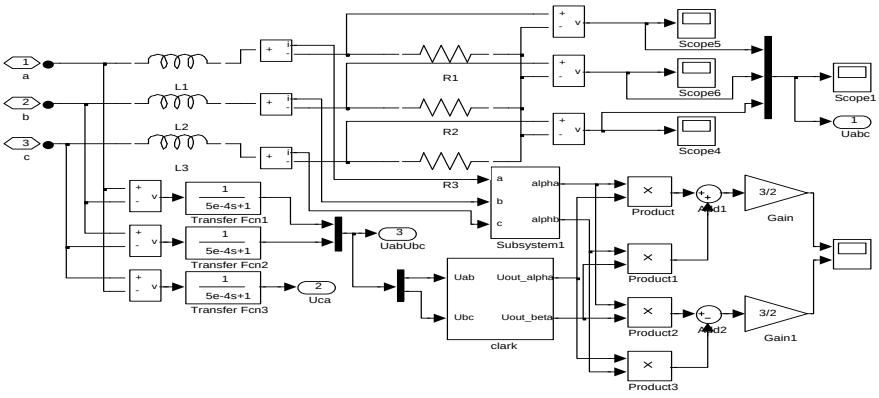

Figure 13. Simulation Diagram of Three-phase Resistance Inductance Load

As shown in Figure 14-16, the simulation analysis is divided into three parts: comparison of input phase current before and after filtering, comparison of grid side power factor before and after adjustment, realization of variable frequency and variable voltage.

In Figure 14, the simulation output frequency is 20Hz, and the input phase currents are PWM waveform with a large number of harmonic components. As Figure 14(b) shows, after filtering, the current harmonic content of the input side is greatly reduced, which is closer to the sine wave, and greatly reduces the harmonic pollution to the grid.

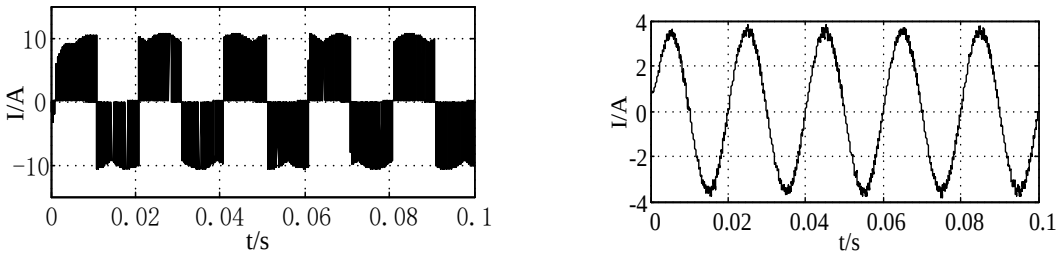

(a) Input phase-current waveform before filtering (b) grid input phase-current waveform after filtering

Figure 14. Input Filter Effects on the Current Waveform

In theory, the output frequency can be any value, during the simulation, the upper limit of the output frequency is 200Hz. As shown in Figure 15(a), (d) and (e), when the output frequency is very low, the required adjustment amplitude is large. When the output frequency is approaching to 50Hz, the required adjustment amplitude is small. When the output frequency exceeds the rated 50 Hz, the grid side power factor decreasing amplitude is small, and the required adjustment amplitude is also small.

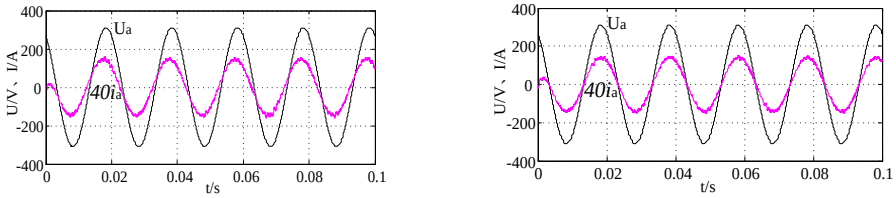

(a) grid side voltage and current waveform before adjustment with the output frequency 20Hz

(b) grid side voltage and current waveform after adjustment with the output frequency 20Hz

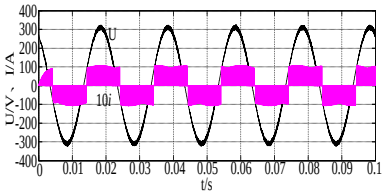

(c) input side voltage and current waveform after adjustment with the output frequency 20Hz

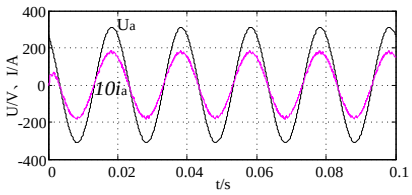

(d) grid side voltage and current waveform before adjustment with the output frequency 50Hz

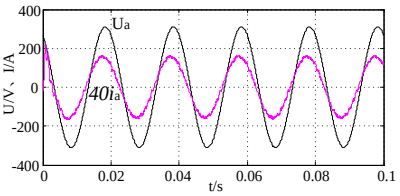

(e) grid side voltage and current waveform before adjustment with the output frequency 200Hz

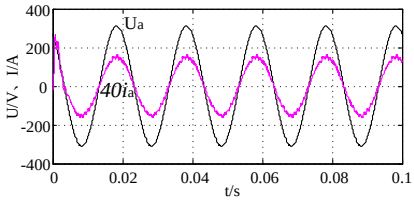

(f) grid side voltage and current waveform after adjustment with the output frequency 200Hz

Figure 15. Grid side Voltage and Current Waveform

As shown in Figure 16(b) and (d), when the output frequency is under 50Hz, the modulation ratio is $m=f_0/50$. When the output frequency is 20Hz, the fundamental wave amplitude of the output line voltage satisfies the formula (13), and the frequency and amplitude is with a linear relationship. As Figure 16(e) and (f) shows, when the output frequency is beyond 50 Hz, set the modulation ratio as m=1, the output line-voltage amplitude under 50Hz is equal to that under 100Hz, which satisfies the formula (13). Thus, it can conclude that voltage amplitude and frequency can change simultaneously. The simulation results verify the validity of the theoretical analysis.

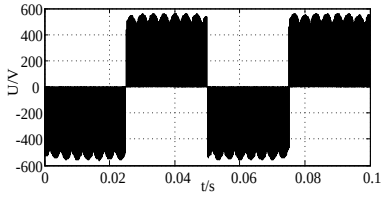

(a) Output line-voltage waveform with the output frequency 20Hz

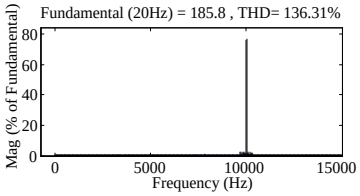

(b) FFT analysis of output line-voltage with the output frequency 20Hz

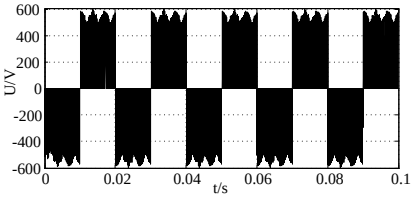

(c) Output line-voltage waveform with the output frequency 50Hz

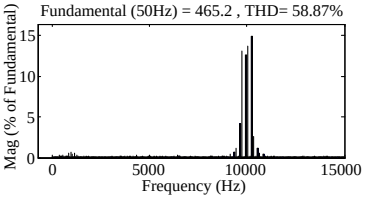

(d) FFT analysis of output line-voltage with the output frequency 50Hz

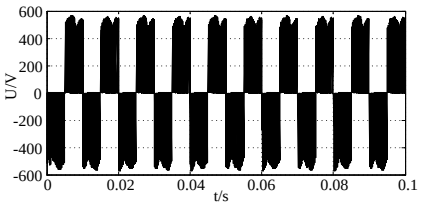

(e) Output line-voltage waveform with the output frequency 100Hz

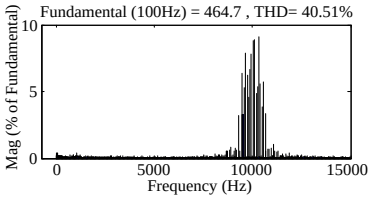

(f) FFT analysis of output line-voltage with the output frequency 100Hz

Figure 16. Output Line-voltage Waveform and FFT Diagram

8. Conclusion

In this paper, theoretical analysis on double SVPWM control of the MC is conducted. Results show that, compared with ordinary PWM converter, the MC has better input-output characteristics. At the same time, a design method of damping input filter is also proposed in this paper, and the adjustment method of the grid side power factor is conducted. At last, system simulations are carried out and the results verify the rationality and validity of the methods described in this paper.

Acknowledgements

This work is supported by the Hei Long Jiang postdoctoral Foundation(LBH-Z10109), HARBIN innovative talent project of science and technology(2014RFXXJ075) and teaching reform project of higher education in Hei Long Jiang Province (JG2014010795).

References

[1] M. Y. Lee, P. Wheeler and C. Klumpner, "Space-vector modulated multilevel matrix converter", IEEE Trans Industrial electronics, vol. 57, no. 10, **(2010)**, pp. 3385-3394.
[2] X. B. Jin, "Research on the SPWM Modulation Strategy in Matrix Converter", 2009 Journal of Harbin University of Science and Technology, vol. 14, no. 4, **(2009)**, pp. 36-40.
[3] H. Cai, H. Lin and Y. C. Yin, "Design of matrix converter input filter and the clamp circuit", Journal of Power Electronics, vol. 41, no. 1, **(2007)**, pp. 23-25.
[4] P. Wheeler and D. Grant, "Optimized input filter design and low-loss switching techniques for a practical matrix converter", IEEE Proceedings. Electric Power Applications, vol. 144, no. 1, **(1997)**, pp. 53-60.
[5] T. Kume, K. Yamada, T. Higuchi, E. Yamamoto, H. Hara, T. Sawa and M. M. Swamy, "Integrated Filters and Their Combined Effects in Matrix Converter", IEEE Trans. Industry Application, vol. 43, no. 2, **(2007)**, pp. 571-581.
[6] M. Su, Y. Sun, H. S. Tan and T. S. Zhang, "Multi-objective optimization design of matrix converter input filter", Proceedings of the CSEE, vol. 27, no. 1, **(2007)**, pp. 70-75.
[7] L. Huber and D. Borojevic, "Space vector modulated three-phase to three-phase matrix converter with Input Power factor correction", IEEE Trans. Industry Applications, vol. 31, no. 6, **(1995)**, pp. 1234-1246.
[8] W. L. Deng, J. L. Zhu and L. T. Zhang, "Optimization algorithm of space vector modulation on matrix converter", Journal of Electric Drive Automation, vol. 25, no. 2, **(2003)**, pp. 25-27.
[9] H. W. She, H. Lin, X. W. Wang and L. M. Yue, "Damped input filter design of matrix converter", Power Electronics and Drive Systems, 2009. PEDS, 2009. International Conference on, **(2009)**, pp. 672-677.
[10] X. N. Lu, K. Sun, G. Li and L. P. Huang, "Analysis and control of input power factor in indirect matrix Converter", Industrial Electronics, 2009. IECON'09. 35th Annual Conference of IEEE, **(2009)**, pp. 207-212.

